applied sciences

MDPI

Article

Integration of an Ultrasonic Sensor within a Robotic End Effector for Application within Railway Track Flaw Detection

Luke Cilia [1], Christian Andrew Griffiths [1], Andrew Rees [2,*] and Jennifer Thompson [1]

[1] Department of Mechanical Engineering, Swansea University, Swansea SA1 8EN, UK; luke.cilia.09@gmail.com (L.C.); c.a.griffiths@swansea.ac.uk (C.A.G.); jennifer.thompson@swansea.ac.uk (J.T.)
[2] Wolfson School, Loughborough University, Loughborough LE11 3TU, UK
* Correspondence: a.rees@lboro.ac.uk

Abstract: The rail industry is constantly facing challenges related to safety with regard to the detection of surface cracks and internal defects within rail tracks. Significant focus has been placed on developing sensor technologies that would facilitate the detection of flaws that compromise rail safety. In parallel, robot automation has demonstrated significant advancements in the integration of sensor technologies within end effectors. This study investigates the novel integration of an ultrasonic sensor within a robotic platform specifically for the application of detecting surface cracks and internal defects within rail tracks. The performance of the robotic sensor system was assessed on a rail track specimen containing sacrificial surface cracks and internal defects and then compared against a manual detection system. The investigation concludes that the robotic sensor system successfully identified internal defects in the web region of the rail track when utilising a 60° and 70° wedged probe, with a frequency range between 4 MHz and 5 MHz. However, the surface crack investigation proved that the transducer was insensitive to the detection of cracks, possibly due to the inadequate angle of the wedged probe. The overall outcome of the study highlights the potential that robotic sensor systems have in the detection of internal defects and characterises the limitations of surface crack identification to assist in enhancing rail safety.

Keywords: flaw detection; rail inspection; robotic system; ultrasonic testing

Citation: Cilia, L.; Griffiths, C.A.; Rees, A.; Thompson, J. Integration of an Ultrasonic Sensor within a Robotic End Effector for Application within Railway Track Flaw Detection. *Appl. Sci.* **2024**, *14*, 1164. https://doi.org/10.3390/app14031164

Academic Editor: Suchao Xie

Received: 15 December 2023
Revised: 18 January 2024
Accepted: 25 January 2024
Published: 30 January 2024

1. Introduction

A statistical analysis presented by the European Union Agency for Railways (ERA) for the years between 2014 and 2018 indicated that broken rail incidents account for almost half of the yearly reported accident precursors [1]. Such incidents have significant impacts, resulting in fatalities, injuries and delays [2]. Fracture mechanics studies have revealed that rail track structural integrity is compromised by the intensive rolling pressure, bending forces and shear stresses they are exposed to during operation [3]. Other factors that contribute to accelerated progressive degradation include cyclic temperature differentials induced by seasonal changes, contact with foreign bodies and undetected fabrication defects [4,5]. Improvements in manufacturing technology have successfully reduced fatigue crack initiation sites [6]. Also, signal-based diagnostic methods have been developed for the purpose of detecting hunting instability incidents [7,8]. However, the ever-increasing demand for additional rail travel has resulted in an increase in axle loads and speed, as well as shorter rail track inspection windows [9,10].

2. State of the Art

Since the 1960s, ultrasound technology has been widely employed as a non-destructive testing (NDT) technology to identify railway flaws [11]. Typically, sub-surface cracks are identified by monitoring the signal strength change in reflected ultrasonic waves via a pulser-receiver system [3]. The instruments employing such technology range from

manual hand-held devices to automated rail cars [12]. The current industry standard utilises fluid-filled ultrasonic wheel probe technology with piezoelectric transducers [13]. The phenomenon of propagation of ultrasonic energy in solid materials, in the form of transverse (shear) waves and longitudinal (compression) waves, compounded with the correlation of the wave's confinement/transmission in the material with wavelength and its exponential decay with depth, are the basis of all the studies related to NDT technology [14]. In 1953, the first Sperry test vehicles were introduced, supplied with ultrasonic transducers for high-speed rail inspection systems [12]. Research dating back to the 1960s shows extensive studies performed on wave-associated displacement profiles and wave scattering in relation to variance in material integrity. Over the years, technology development led to the two typical configurations of ultrasonic transducer inspection methods: the pitch-catch and the pulse-echo. The pitch-catch configuration comprises a separate actuator and sensor, whereas when using the pulse-echo method, the transducer acts as both the actuator and sensor. Typically, pulse-echo transducers are applied for the detection of sub-surface flaws, while pitch-catch transducers are used for the detection of cracks/discontinuities such as vertical splits (parallel to the rail length) [15]. For both transducer configurations, to aid wave transfer between the sensor and rail track, a liquid-based couplant is required.

In 1967, Viktorov proposed measuring the change in period of oscillation in the frequency domain to determine the defect depth [16]. This approach was enhanced further by Domarkas et al. and Hall et al., whose research facilitated the determination of defect length via pulse time measurement [17,18]. In the research conducted by Papaelias et al., it was concluded that defect detection is optimised when transmitting ultrasound waves at incident angles of 0°, 37°, 45° and 70° [19]. This approach makes ultrasonic flaw detection highly efficient, especially in recognising deep internal defects, particularly those located in the rail head, web and foot regions. However, the configuration is less efficient for identifying rolling contact fatigue defects typically located closer to the surface (<4 mm deep) [19]. Researchers have investigated the effect of frequency during laser-generated ultrasound. Frequency analysis studies have indicated that frequencies between 0.4 and 3 MHz used in combination with a high-order wave are suitable for the measurement of the cold work layer and stress measurements [12,20,21]. Pecoraci et al. and Grewal also analysed the resulting ageing process in steel and defect flaws through examining changes in wave velocity and attenuation of high-frequency waves above 1 MHz [22,23]. In a study by Rizzo et al., the limitation of high-frequency analysis for the application of deep detection of flaws was identified and attributed to a lack of sensitivity at deeper defect depths [24]. In a further study by Achenbach, it was found that frequencies of 2 MHz are effective for defect detection to a depth of 0.75 mm. However, at lower frequencies of 150 kHz, defects can be identified at depths of 10 mm [22]. Low-frequency waves, however, can experience a loss of resolution [25]. In particular, in a study by Bartoli et al., it was observed that when analysing defects that measure 15% of the rail head section, reflections are identified when using a 20–45 kHz frequency range [25].

The advancements in the data collection and subsequent data interpretation allow for the rapid geometry detection and visualisation of wave propagation diffraction when utilising ultrasound inspection methods [6]. Also, enhancements in sensor technology, robotics and artificial intelligence have made the introduction of robots in the railway industry more appealing [26].

Gowtham et al. developed an automated robotic inspection system for the application of detecting and measuring cracks in rail tracks [26]. To date, there has only been limited research into the novel concept of integrating sensors within robotic end effectors. One such study that has been investigated evaluated the use of a 2D vision camera and 3D laser line scanner to identify and locate areas requiring repair on a rail track specimen [27].

Within the context of automated sensing, this investigation integrates an ultrasonic detection technology, Epoch™ 650, with an automated robotic system, KUKA KR 16, specifically for the enhanced detection of railway track flaws. To provide an informed assessment of the developed system, a comparison was experimentally performed via a

direct manual-use system. This work is a starting point for the creation of a knowledge repository for the enhancement of rail safety via automated railway track inspection. The paper is organised as follows. Section 3 presents the experimental procedure. In Section 4, the experimental results are presented. Section 5 presents a discussion on the suitability of the system to detect flaws. Finally, in Section 6, the main conclusions from the conducted study are presented.

3. Experimental Set-Up

In this research, an ultrasonic sensor, Epoch™ 650, was integrated within the end effector of a KUKA KR 16 robotic system to compare its efficacy against a manual process. To assess the performance of the novel system, sacrificial holes (internal defects) and slots (surface cracks) were machined into a steel railway track specimen of grade R260 (Figure 1). The sacrificial features were machined via wire electrical discharge machining, and the flaws ran through the full height of the track (Figure 2). The details of these features are presented in Table 1.

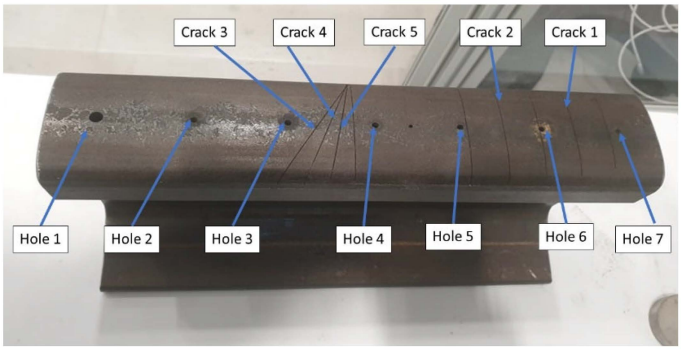

Figure 1. Railway track test piece.

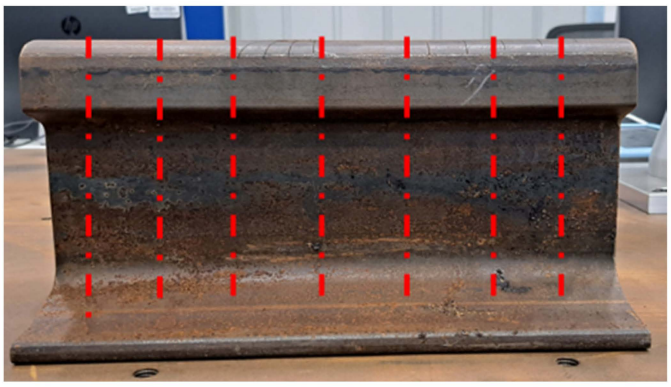

Figure 2. Test piece scanning direction.

Table 1. Test piece features details.

Fault Type	Position (mm)	Surface Length (mm)	Depth (mm)	Fault Angle (°)	Scanning Position
Crack 1	90	72	8	-	1
Crack 2	110	74	10	-	1
Crack 3	170	75	13	10	1
Crack 4	170	75	15	20	1
Crack 5	170	75	18	30	1

Table 1. *Cont.*

Fault Type	Position (mm)	Surface Length (mm)	Depth (mm)	Fault Angle (°)	Scanning Position
Hole 1	22	6 (Ø)	Through	-	2
Hole 2	62	3 (Ø)	Through	-	2
Hole 3	113	2.5 (Ø)	Through	-	2
Hole 4	156	3 (Ø)	Through	-	2
Hole 5	204	2.5 (Ø)	Through	-	2
Hole 6	246	3 (Ø)	Through	-	2
Hole 7	293	3 (Ø)	Through	-	2

The Epoch™ 650 used in this study utilises a piezoelectric transducer with an integrated receiver to propagate ultrasonic energy into the specimen. The selected Angle Beam Wedge Transducers are single-element transducers used for flaw detection and sizing. The unit transmits a primary shear wave into a test piece and the design allows it to be easily scanned back and forth over the inspected part. This is unlike straight-beam testing, where the sound beam will travel at the generated angle down to the bottom of the test piece and then be reflected upward at the same angle. In selected-angle beam testing, by moving the probe back and forth, the sound beam will sweep across the full height of a detected flaw. This scanning motion enables the inspection of the entire flaw either through direct reflection from a second acoustic path (Figure 3a,b) or through a second acoustic path (Figure 3c,d). These transducers are typically used for the inspection of welds and of cracks on pipes, tubes, forgings, castings and machined components. They are Atlas European Standard Transducers, designed to meet inspection criteria referenced throughout Europe, and feature standard connectors and common frequencies. The two sensors use a 70- and 60-degree refracted shear wave (frequency range between 4 MHz and 5 MHz) and have a near-field distance in steel of 30 mm. Before inspection, both sensors were tested using NDT Calibration and Reference Test Blocks. The blocks used were a U8880016 2214M 5-STEP 1018 steel block and a U8880046 TB1065-1 ISO 7963 miniature steel block (ISO 7963 Ultrasonic testing).

For both the automated robotic and manual experiments, the rail specimen was studied by running the probe along the centre of the head of the rail, specifically to investigate the surface cracks (Figure 4a). Subsequently, the web region (Figure 4b) was scanned for the internal defects created in the form of holes. Both scanning approaches were carried out at a low speed in the direction observed in Figure 5. Glycerin was applied as a couplant between the transducer and the test piece to facilitate more efficient sound transmission and a stronger signal strength. The probe was held stationary when the known flaws were located to allow the successive generation of data. The data collected from the Epoch™ 650 are presented in a graphical A-Scan waveform display. The pulse travel time is depicted in the horizontal direction, whilst the echo amplitude is depicted in the vertical direction [28]. The system adopted allowed the amplification of the signals of interest and manipulation of the time base to permit focusing on the area containing flaws. Furthermore, the waveform-averaging software allowed the calculation of an average of the successively acquired A-scans, which improved the sign-to-noise ratio on detection of the static flaws [28]. For the automated robotic experiment, the ultrasonic probe was located within a universal gripper housing that is compatible with the use of angled probes (Figure 6a).

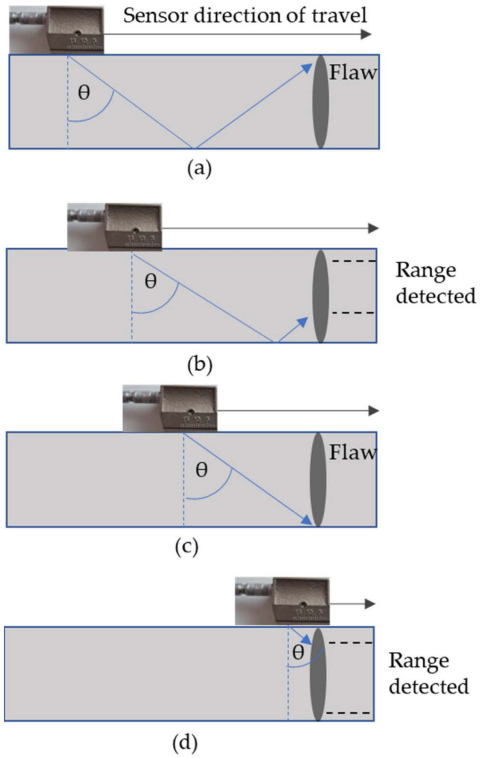

Figure 3. Test piece scanning approach for rail track head (**a**,**c**) and web (**b**,**d**).

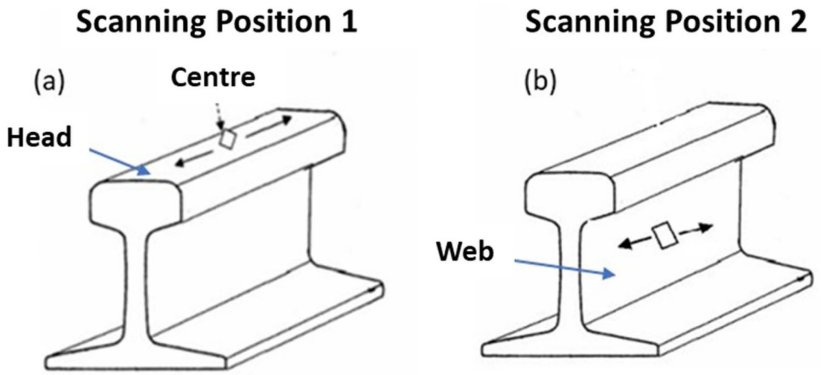

Figure 4. Test piece scanning approach for rail track head (**a**) and web (**b**).

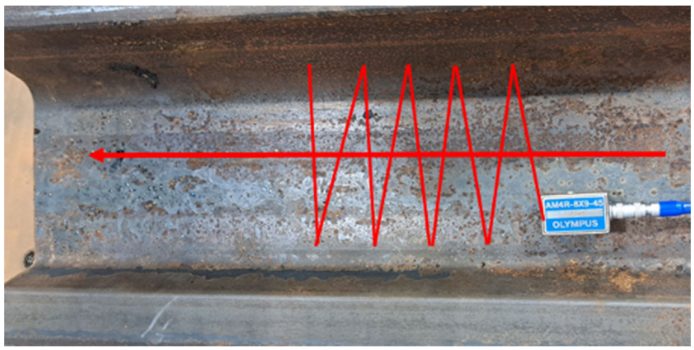

Figure 5. Test piece scanning approach for rail track head and web.

(**a**) (**b**)

Figure 6. (**a**) Automated robotic testing system and (**b**) manual testing system.

3.1. Sensor Calibration

Calibration of the Epoch™ 650 ultrasonic flaw detector and of the angled probe was required to identify defects within a specimen sample of the specific material. The main test piece used for calibration was a steel test bar with machined slots across the face of the material, perpendicular to the sample surface. The depths of the slots on the calibration block varied from 2.5 mm to 12.5 mm. The sound velocity penetrating the material via the transducer was set between 5850 and 5890 ms^{-1}. In addition, the parameters of range, frequency and damping were aligned to the R260-grade steel test piece [29].

The transducer angle of 60° or 70° was selected by measuring the thickness of the web of the material (20 mm). Based on the literature, wedged angles less than 45° are generally only used when the thickness of the metal exceeds 50 mm [29]. A calibration of the distance gain size (DGS) function was also conducted. The calibration was conducted by coupling the transducer to the calibration block and obtaining a reference reflection based on known geometries and sizes within the calibration steel test bar. The Epoch™ 650 then generated DGS curves based on the relevant reflection profile in the form of level amplitude. A transfer correction value, referred to as Delta VT, was also set up to compensate for amplitude differences from the surface variance between the calibration block and the test sample. During the experiment, this was the basis on which the sizing of the detected flaws was mathematically calculated. The amplitude of the echo from the defects of the specimen sample were compared and related to the equivalent DGS curve, obtained from the reference reflectors [28].

3.2. Experimental Procedure

For both the automated robotic and manual experiments, the rail track specimen was positioned beneath the sensor as illustrated in Figure 6a,b. The probe scanning process was performed at a speed of approximately 6 mm/sec. To assess the repeatability of the experiment, each test was conducted three times.

4. Results

4.1. Surface Cracks

The experiments on the surface cracks were conducted by running the scanning probe along the centre of the rail head, as depicted in Figure 4a. For both the automated robotic and manual system configurations, none of the surface cracks listed in Table 1 were detected by the 60° and 70° wedged probes at any frequency between 4 MHz and 5 MHz.

4.2. Internal Defects

The experiments on internal defects were conducted by running the scanning probe along the web region. For both the automated robotic and manual system configurations, a clear distinction could be witnessed between clear regions and defect regions in the resulting A-scan image amplitude, as evidenced in Figure 7. In Figure 7a, no signal is present (no green spiked peak), meaning that in that specific region, there are no cracks. Figure 7b,c both show a signal (a green distinct peak), and this is observed when using the probe manually and when using the robotic configuration, therefore proving that cracks can be detected both manually and automatically.

(**a**) (**b**) (**c**)

Figure 7. (**a**) A-Scan image, 60° probe, no flaw region. (**b**) A-Scan image, 60° probe, defect region, manual configuration. (**c**) A-Scan image, 60° probe, defect region, robotic configuration.

Importantly, in both the manual and robotic configurations, all the defects were identified by a clear change in signal; specifically, higher amplitudes were observed in regions with defects. The Epoch™ 650 system compared the signal amplitude obtained via the calibration data and identified the corresponding depth of the defect. This confirmed the effectiveness of both systems in successfully detecting the hole defects by scanning along the web region.

After running the full cycle of tests for both configurations, all DGS data were recorded. Results generated for holes of the same size were clustered to assess repeatability and statistical significance. Internal defects were clustered as holes with a diameter of 2.5 mm, 3 mm and 6 mm.

A One-Sample T-test was conducted to compare the mean sample defect size data of each system configuration (manual 60° wedge, robotic 60° wedge, manual 70° wedge and robotic 70° wedge) against the actual defect size. Also, the standard deviation, mean and two-sided probability value (p-value) were also calculated. For the manual system measurements, correlations to the actual defect sizes were obtained for all hole sizes when using both angled wedged probes. For the robotic system measurements, correlation to the actual defect size was only witnessed on the 3 mm hole cluster when using the 60° wedged probe. However, when using the 70° wedged probe, all hole sizes were correctly identified. The subsequent p-value (set at 0.05) statistical analysis of the mean values obtained from the experiments concluded that all internal defect measurements corresponded well to the actual values. This confirmed that the size characterisation of internal defects was attainable by both the robotic and manual system, with the robotic system showing slightly less consistency and accuracy when adopting the 60° wedged probe.

Figure 8 displays the T-test analysis comparing the mean DGS values from the manual and automated configurations when utilising the 60° and 70° probes independently. Marginally lower variance was witnessed between the manual and robotic configurations when analysing the 2.5 mm and 3 mm defects with the 70° probe. In particular, the resultant p-value exceeded the 0.05 level of significance, as displayed in Table 2. However, for the 6 mm defect, the difference between the two probes was indicated as being significant in both systems, as shown in Table 2. Overall, the accuracy for both the robotic and manual configurations was higher when using the 60° and 70° wedged probes to analyse the 2.5 mm and 3 mm defect sizes.

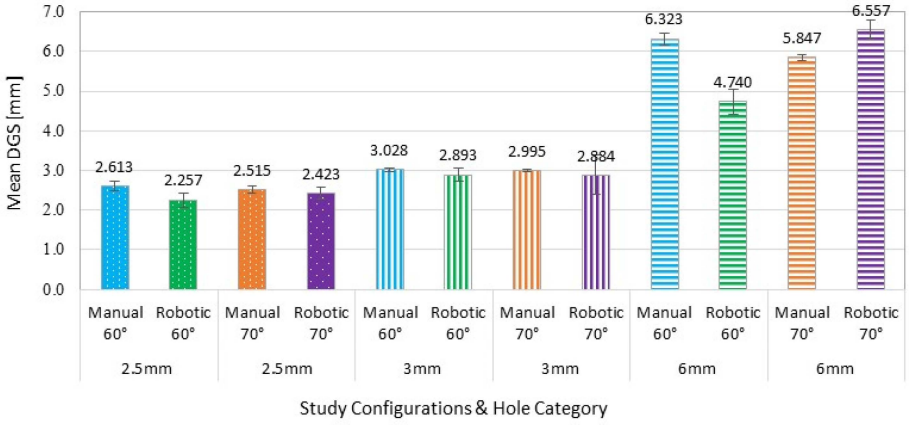

Figure 8. Comparison of the mean DGS reading from all experiments (blue—Manual 60°; green—Robotic 60°; orange—Manual 70°; purple—Robotic 70°; dots—2.5 mm; vertical lines—3 mm; horizontal lines—6 mm).

Table 2. Independent T-test data for 2.5 mm, 3 mm and 6 mm.

Study	Mean Defect Size	STD. Deviation	*p*-Value
For the 2.5 mm defect			
Manual 60°	2.613	0.118	0.124
Manual 70°	2.515	0.082	0.124
Robotic 60°	2.257	0.176	0.101
Robotic 70°	2.423	0.141	0.101
For the 3 mm defect			
Manual 60°	3.028	0.046	0.066
Manual 70°	2.995	0.035	0.066
Robotic 60°	2.893	0.175	0.952
Robotic 70°	2.884	0.494	0.952
For the 6 mm defect			
Manual 60°	6.323	0.147	0.008
Manual 70°	5.847	0.081	0.008
Robotic 60°	4.740	0.316	0.001
Robotic 70°	6.557	0.235	0.001

The second dependent variable that was compared was the recorded sound path, which indicates the depth and location of the internal defect. An Independent Samples *T*-test analysis comparing the manual and robotic configurations for the 60° and 70° probes separately indicated that there was no significant difference for this parameter in the 2.5 mm and 3 mm defect categories, as well as for the readings obtained by the 60° probe for the 6 mm hole (Figure 9). The only significant difference observed was for the 70° probe in the 6 mm defect category. These results further confirm the comparability between the manual and the robotic system. In conclusion, the overall results of the study show the high potential of the robotic system coupled with the ultrasonic flaw detector system for rail defect detection and localisation.

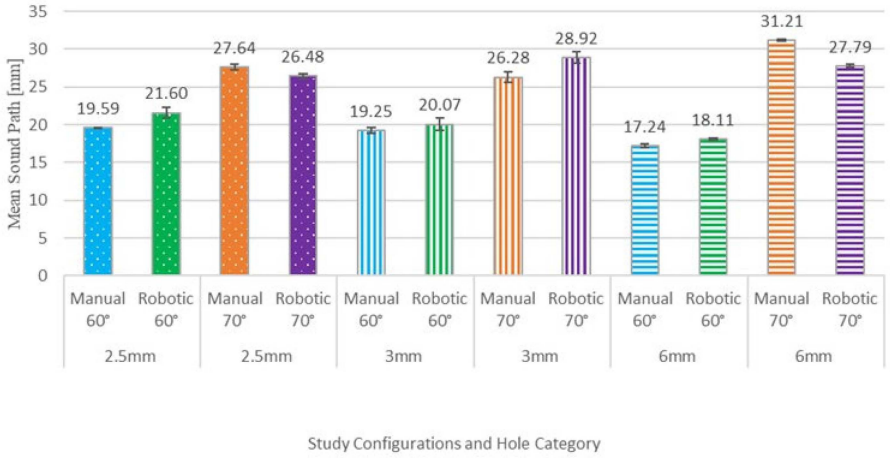

Figure 9. Comparison of the mean sound path DGS from all experiments (blue—Manual 60°; green—Robotic 60°; orange—Manual 70°; purple—Robotic 70°; dots—2.5 mm; vertical lines—3 mm; horizontal lines—6 mm).

5. Discussion

This study presents additional insight into the potential of railway track flaw detection through the use of robotics for the application of enhanced rail safety. Initial results generated for the surface crack study demonstrated that the transducer was insensitive to the detection of surface cracks. This observation can be supported by the investigation by Kurokawa and Inoue, who concluded that when using conventional probes, high frequencies in the range of 5 MHz result in a higher resolution. Shorter wavelengths increase the sensitivity of the system to any small inhomogeneity, such as the rough surface of the cracks or crystal grains in the material [30]. Therefore, as the tests within this investigation were performed using a frequency between 4 MHz and 5 MHz, this could have been a plausible explanation for increased wave scattering, thereby resulting in poor data-capture performance. However, previous studies have demonstrated that using a wedged probe compensates for increased scattering by providing a delay line and an angled incident wave [31]. Although wedged probes were used within this study, the results demonstrate that the both the automated robotic and manual systems are not appropriate for surface crack detection.

The underlying cause of these adverse results is substantiated by studies indicating that conventional ultrasonic testing is very challenging when used as a tool to inspect cracks close to the surface. This is due to the existence of an area referred to as the 'dead zone'. Defect-deflected echoes located a few millimetres in front of the transducer were found to be overshadowed by disturbing signals caused by the piezoelectric element ringing inside the transducer [32]. Anandika mitigated this issue by adopting a wedged phased-array technique [31]. Unlike a conventional ultrasound's single fixed-angle element (determined by the wedge), the advantage associated with the array phase system is that it utilises beam steering to create beams at multiple angles, allowing multi-angular defect testing via a single probe [33]. In this way, the location of the noise signals with respect to the surface defect position shifts, thereby increasing the probability of detection of the surface anomalies. Furthermore, it offers the advantage of a far more effective spatial sampling frequency, thereby increasing the scanning efficiency [31]. Considering these findings, repeating the investigation with a 90° wedged probe might result in a different outcome. The angle of inclination of the wave would generate a surface wave, producing a stronger reflected echo from the surface defects, which suppresses the unwanted modes in the 'dead zone' [34].

The investigation of the web region of the railway track confirmed that both the automated robotic and manual systems could successfully detect internal defects in the form of holes ranging from 2.5 to 3 and 6 mm. Furthermore, low variance was observed between

the sacrificial defect size and the mean DGS measured by both configurations. The findings related to the manual system suggest that the flaw detector with set parameters provided a reliable means for measuring the defect size. The proposed robotic configuration, specifically with the 70° wedged probe, was also found to be effective at accurately measuring the defect size. Furthermore, the mean DGS readings were also similar to those generated by the manual system. Extending the study to measure a range of defect sizes in different orientations, and scanning in different directions, would provide further insight into the effectiveness of the proposed robotic system for use in scanning actual rails.

Characterisation data obtained via the 60° and 70° wedged probes for the manual and robotic configurations demonstrated consistency (Table 2). Any variances observed could be attributed to human error, primarily skill-based errors, which further demonstrates the enhanced consistency that can be obtained from automated robotic systems. During the manual experiment, it was observed that the highest peak values fluctuated easily with the slightest shift in movement. The difference in screening speed over the rail was another variable which could have caused measurement discrepancies. However, this was mitigated by adopting a programmed path in the robotic system which moved at a constant slow speed. The robotic system offered this advantage over the manual system.

Another successful parameter for which the robotic system was found to be equivalent to the manual configuration was the measurement of internal defect depth/surface distance. Sound path data generated for the localisation of the defects were mostly comparable for both configurations. This similar performance of both experimental set-ups offers significant potential for future testing and the development of detection systems. The literature suggests that the key challenge when using the ultrasound measuring system is the constant need to maintain contact with the couplant and with the rail specimen [27]. However, with the introduction of automation and robotics, the possibility of improper contact was negligible, since the motion system was calibrated and the trajectory was programmed, offering a marginal possibility of error (<0.9 mm). Furthermore, the possibility of human error was also reduced.

6. Conclusions

Within the context of automated sensing, this investigation integrates the novel integration of an ultrasonic detection technology, Epoch™ 650, within the end effector of a KUKA KR 16 robotic system specifically for the application of the enhanced detection of railway track flaws. To provide an informed assessment of the developed system, a comparison was performed via a manual system. The main conclusions derived from the study are the following:

- Both the manual and robotic configurations were proven to be ineffective at detecting surface crack defects when employing the 60° and 70° wedged probe.
- Both configurations were effective at detecting internal rail defects, perpendicular to the direction of the propagated incident ultrasonic wave, located in the web region of the rail.
- The characterization of internal defects by the robotic system with a speed of 6 mm/s was comparable to the actual defect size and to the values attained by the manual approach.
- Depth and location measurements of the internal flaws were shown to be comparable for both systems.

This research was focused on the hypothesis that automation is viable for detecting flaws on rail tracks. Future research should now focus on the design of end effectors that can accommodate multi-transducers for increased ultrasonic testing. In addition, an end effector design that can accommodate a phased-array (PA) transducer should be studied. Compared with single-element systems, the PA uses a total focusing method (TFM) that provides full matrix capture (FMC). This would make the mapping of tracks much easier and more accurate than with traditional ultrasonic equipment.

Author Contributions: Writing—original draft, L.C.; Writing—review & editing, A.R. and J.T.; Supervision, C.A.G. All authors have read and agreed to the published version of the manuscript.

Funding: This research received no funding.

Institutional Review Board Statement: Not applicable.

Informed Consent Statement: Not applicable.

Data Availability Statement: The data presented in this study are available on request from the corresponding author.

Acknowledgments: The authors would like to acknowledge the support of the Department of Mechanical Engineering, Future Manufacturing Research Institute, Faculty of Science and Engineering, Swansea University, and the Advanced Sustainable Manufacturing Technologies (ASTUTE 2022) project, in enabling the research upon which this paper is based. Further information on ASTUTE can be found at www.astutewales.com and https://www.swansea.ac.uk/science-and-engineering/research/engineering/astute/ (accessed on 29 January 2014).

Conflicts of Interest: The authors declare no conflict of interest.

References

1. European Union Agency for Railways. *Report on Railway Safety and Interoperability in the EU, 2020*; European Union Agency for Railways: Luxembourg, 2020; Available online: https://www.era.europa.eu/sites/default/files/library/doc/safety_interoperability_progress_reports/report_on_railway_safety_and_interoperability_in_the_eu_2020_en.pdf (accessed on 15 October 2021).
2. Bombarda, D.; Vitetta, G.M.; Ferrante, G. Rail Diagnostics Based on Ultrasonic Guided Waves: An Overview. *Appl. Sci.* **2021**, *11*, 1071. [CrossRef]
3. Ge, H.; Huat, D.C.K.; Koh, C.G.; Dai, G.; Yu, Y. Guided wave–based rail flaw detection technologies: State-of-the-art review. *Struct. Health Monit.* **2021**, *21*, 1287–1308. [CrossRef]
4. Won Park, J.; Gyu Lee, T.; Chul Back, I.; Jun Park, S.; Min Seo, J.; Jae Choi, W.; Gon Kwon, S. Rail Surface Defect Detection and Analysis Using Multi-Channel Eddy Current Method Based Algorithm for Defect Evaluation. *J. Nondestruct. Eval.* **2021**, *40*, 83. [CrossRef]
5. Cannon, D.F.; Edel, K.O.; Grassie, S.L.; Sawley, K. Rail defects: An overview. *Fatigue Fract. Eng. Mater. Struct.* **2003**, *26*, 865–886. [CrossRef]
6. Hesse, D. Rail Inspection Using Ultrasonic Surface Waves. Ph.D. Thesis, Imperial College University of London, London, UK, 2007.
7. Kulkarni, R.; Qazizadeh, A.; Berg, M.; Carlsson, U.; Stichel, S. Vehicle running instability detection algorithm (VRIDA): A signal based onboard diagnostic method for detecting hunting instability of rail vehicles. *Proc. Inst. Mech. Eng. Part F J. Rail Rapid Transit* **2022**, *236*, 262–274. [CrossRef]
8. Zeng, Y.; Zhang, W.; Song, D. A new strategy for hunting alarm and stability evaluation for railway vehicles based on nonlinear dynamics analysis. *Proc. Inst. Mech. Eng. Part F J. Rail Rapid Transit* **2020**, *234*, 54–64. [CrossRef]
9. Peterson, M.L.; Jeffrey, B.D.; Gutkowski, R.M. Limitations in size and type of detectable defects in rail flaw inspection. *Insight-Non-Destr. Test. Cond. Monit.* **2000**, *42*, 306–311.
10. Wu, F.; Xie, X.; Guo, J.; Li, Q. Internal Defects Detection Method of the Railway Track Based on Generalization Features Cluster. Research Gate. *Res. Sq.* **2021**. *preprint*. [CrossRef]
11. Allison, A.B. Sperry rail service. *Bull. Natl. Railw. Hist. Soc.* **1968**, *33*, 7–21.
12. Bray, D.E. Historical review of technology development in NDE. In Proceedings of the 15th World Conference on NDT, Rome, Italy, 15–21 October 2000.
13. Fadaeifard, F.; Toozandehjani, M.; Mustapha, F.; Matori, K.A.B.; Arrafin, M.; Zahari, N.I.; Nourbakhsh, A.A. Rail inspection technique employing advanced nondestructive testing and Structural Health Monitoring (SHM) approaches—A review. In Proceedings of the Malaysian International NDT Conference and Exhibition (MINDTCE 13), Kualalampur, Malaysia, 17–18 June 2013.
14. Rayleigh, L. On waves propagated along the plane surfaces of an elastic solid. In Proceedings of the London Mathematical Society, London, UK, 12 November 1885.
15. Rowshandel, H. The Development of an Autonomous Robotic Inspection System to Detect and Characterise Rolling Contact Fatigue Cracks in Railway Track. Ph.D. Thesis, University of Birmingham, Birmingham, UK, 2013.
16. Viktorov, I.A. *Rayleigh and Lamb Waves: Physical Theory and Applications*; Springer: New York, NY, USA, 1967.
17. Hall, K.G. Crack depth measurement in rail steel by Rayleigh waves aided by photoelastic visualisation. *Non-Destr. Test.* **1976**, *9*, 121–126. [CrossRef]
18. Domarkas, V.; Khuri-Yakub, B.T.; Kino, G.S. Length and depth resonances of surface cracks and their use for crack size estimation. *Appl. Phys. Lett.* **1978**, *33*, 557–559. [CrossRef]

19. Papaelias, M.P.; Roberts, C.; Davis, C.L. A review on non-destructive evaluation of rails: State-of-the-art and future development. *Proc. Inst. Mech. Eng. Part F J. Rail Rapid Transit* **2008**, *222*, 367–384. [CrossRef]
20. Egle, D.M.; Bray, D.E. Measurement of acoustoelastic and third-order elastic constants for rail steel. *J. Acoust. Soc. Am.* **1976**, *60*, 741–744. [CrossRef]
21. Hirao, M.; Kyukawa, M.; Sotani, Y.; Fukuoka, H. Rayleigh wave propagation in a solid with a cold-worked surface layer. *J. Nondestruct. Eval.* **1981**, *2*, 43–49. [CrossRef]
22. Grewal, D.S. Improved ultrasonic testing of railroad rail for transverse discontinuities in the rail head using higher order Rayleigh (M21) waves. *Mater. Eval.* **1996**, *54*, 983–986.
23. Pecorari, C.; Gros, X.; Acosta, B.; Debarberis, L.; Beers, M.; Manna, G. Assessment of Steels ageing by Rayleigh wave velocity measurements. In Proceedings of the 15th World Conference on Nondestructive Testing, Rome, Italy, 15–21 October 2000.
24. Rizzo, P.; Cammarata, M.; Bartoli, I.; Scalea, F.L.D.; Salamone, S.; Coccia, S.; Phillips, R. Ultrasonic Guided Waves-Based Monitoring of Rail Head: Laboratory and Field Tests. *Adv. Civ. Eng. Vol.* **2010**, *2010*, 291293. [CrossRef]
25. Bartoli, I.; Scaleaa, F.L.D.; Fatehb, M.; Viola, E. Modeling guided wave propagation with application to the long-range defect detection in railroad tracks. *NDT E Int. Indep. Nondestruct. Test. Eval.* **2005**, *38*, 325–334. [CrossRef]
26. Gowtham, P.; Mahendar, R.; Aravind, R.; Ganesh, K.S. Smart robot for rail track flaw detection using NDT. *Int. J. Adv. Res. Biol. Eng. Sci. Technol.* **2016**, *2*, 122–127.
27. De Becker, D.R. The Use of Hybrid Manufacturing in the Repair and Maintenance of Railway Lines. Ph.D. Thesis, Loughborough University, Loughborough, UK, 2020.
28. Olympus. *Epoch 650 Ultrasonic Flaw Detector—User's Manual*; Olympus: Westborough, MA, USA, 2015.
29. Olympus Europa. *Olympus—Evident. Ultrasonic Flaw Detection Tutorial: 6.2 Angle Beam Probe Selection*; Olympus Europa: Hamburg, Germany, 2015; Available online: https://www.olympus-ims.com/en/ndt-tutorials/flaw-detection/angle-beam-probe-selection/ (accessed on 12 April 2022).
30. Kurokawa, Y.; Inoue, H. Development of Flaw Visualization Technique at Near Field of Phased Array Probe. *J. Solid Mech. Mater. Eng.* **2010**, *4*, 1654–1663. [CrossRef]
31. Anandika, R. Non-Destructive Measurements of Near-Surface Cracks in Railheads. Ph.D. Thesis, Lulea University of Technology, Luleå, Sweden, 2021.
32. Moon, H.J.; Seung, H.M.; Choi, W. Autoencoder-based detection of near-surface defects in ultrasonic testing. *Ultrasonics* **2022**, *119*, 106637.
33. Olympus. *Phased Array Testing: Basic Theory for Industrial Applications*; NDT Field Guides; Olympus Scientific Solutions: Waltham, MA, USA, 2014; Available online: https://www.academia.edu/40766556/Phased_Array_Testing_Basic_Theory_for_Industrial_Applications (accessed on 4 April 2022).
34. Baishya, C.; Saxena, B.; Bhattacharya, V.; Vijay, R. *Ultrasonics in Railways*; Metallurgical & Chemical Directorate: Jamshedpur, India, 2008.